TMS-evoked potential propagation reflects effective brain connectivity

Daly, I. ORCID: https://orcid.org/0000-0001-5489-0393, Williams, N. ORCID: https://orcid.org/0000-0002-0719-4616 and Nasuto, S. J. ORCID: https://orcid.org/0000-0001-9414-9049 (2024) TMS-evoked potential propagation reflects effective brain connectivity. Journal of Neural Engineering, 21 (6). 066038. ISSN 1741-2552 doi: 10.1088/1741-2552/ad9ee0 Available at https://centaur.reading.ac.uk/120553/

TMS-evoked potential propagation reflects effective brain connectivity

Journal of Neural Engineering

PAPER

TMS-evoked potential propagation reflects effective brain connectivity

Ian Daly[1,*], Nitin Williams[2,3] and Slawomir J Nasuto[4,*]

[1] Brain-Computer Interfacing and Neural Engineering Laboratory, School of Computer Science and Electronic Engineering, University of Essex, Colchester, United Kingdom
[2] Department of Neuroscience & Biomedical Engineering, Aalto University, Espoo, Finland
[3] Department of Computer Science, University of Helsinki, Helsinki, Finland
[4] Biomedical Sciences and Biomedical Engineering Division, School of Biological Sciences, University of Reading, Reading, United Kingdom
[*] Authors to whom any correspondence should be addressed.

E-mail: i.daly@essex.ac.uk and s.j.nasuto@reading.ac.uk

Keywords: brain connectivity, TMS, TEP, MVAR, EEG

OPEN ACCESS

RECEIVED
12 January 2024

REVISED
19 November 2024

ACCEPTED FOR PUBLICATION
13 December 2024

PUBLISHED
27 December 2024

Abstract

Objective. Cognition is achieved through communication between brain regions. Consequently, there is considerable interest in measuring effective connectivity. A promising effective connectivity metric is transcranial magnetic stimulation (TMS) evoked potentials (TEPs), an inflection in amplitude of the electroencephalogram recorded from one brain region as a result of TMS applied to another region. However, the TEP is confounded by multiple factors and there is a need for further investigation of the TEP as a measure of effective connectivity and to compare it to existing statistical measures of effective connectivity. *Approach.* To this end, we used a pre-existing experimental dataset to compare TEPs between a motor control task with and without visual feedback. We then used the results to compare our TEP-based measures of effective connectivity to established statistical measures of effective connectivity provided by multivariate auto-regressive modelling. *Main results.* Our results reveal significantly more negative TEPs when feedback is not presented from 40 ms to 100 ms post-TMS over frontal and central channels. We also see significantly more positive later TEPs from 280–400 ms on the contra-lateral hemisphere motor and parietal channels when no feedback is presented. These results suggest differences in effective connectivity are induced by visual feedback of movement. We further find that the variation in one of these early TEPs (the N40) is reliably related to directed coherence. *Significance.* Taken together, these results indicate components of the TEPs serve as a measure of effective connectivity. Furthermore, our results also support the idea that effective connectivity is a dynamic process and, importantly, support the further use of TEPs in delineating region-to-region maps of changes in effective connectivity as a result of motor control feedback.

1. Introduction

Cognition is achieved through communication between specialised brain regions (Sporns 2007). Hence, a considerable portion of Cognitive Neuroscience research is devoted to mapping these patterns of communication (referred to as brain connectivity), and relating them to different cognitive tasks (Murre and Sturdy 1995, Rubinov and Sporns 2009, Raichle 2011).

Brain connectivity is typically measured via functional connectivity or effective connectivity (Sporns 2007). While functional connectivity refers to purely statistical relationships between neural activity in different brain regions (Raichle 2011), effective connectivity refers to measures of causal relationships between brain regions (Murre and Sturdy 1995, Sporns 2007, Arai *et al* 2012). For example, if changes in neural activity in region A of the brain produce a change in activity in region B of the brain, we can

infer a causal relationship from region A to region B. In other words, brain region A is exhibiting effective connectivity with brain region B. These relationships are most typically measured via statistical metrics of connectivity such as multivariate auto-regressive (MVAR) modelling.

Perturbation-based methods are an alternative promising approach to estimating effective connectivity between brain regions (Lepage *et al* 2013, Kafashan *et al* 2014). Perturbation-based measurements of causality are achieved by perturbing process A and observing process B, to see if the perturbation of process A produces a change in process B. Due to its fine spatial resolution, transcranial magnetic stimulation (TMS) (Hallett 2000, 2007) has been proposed to apply a focused magnetic field as a perturbation, with electroencephalogram (EEG) being used to measure resulting changes in brain activity (Ilmoniemi *et al* 1997). Consequently, it has been suggested that effective connectivity between the stimulated brain region and other brain regions can be estimated by measuring motor evoked potential (MEP) relationships to brain states (Ferreri *et al* 2011, Rothwell 2011, Daly *et al* 2018, Schaworonkow *et al* 2019) and that this depends on ongoing changes in the phase of neural activity (Keil *et al* 2014). For example, paired pulse TMS is widely used to probe connectivity between the motor site M1 and other areas of the brain by first stimulating the area of interest, followed by stimulating M1 and then measuring the resulting MEP, which serves as a correlate of the connectivity between the area of interest and M1 (Ziluk *et al* 2010, Breveglieri *et al* 2021). Additionally, it has been suggested that effective connectivity may also be estimated by measuring transcranial evoked potentials (TEPs) in the EEG (Ilmoniemi *et al* 1997, Granö *et al* 2022). Specifically, TEPs have been proposed to measure effective connectivity between brain region A (the site of the stimulation) and all other brain regions positioned underneath the EEG electrodes (Hallett *et al* 2017).

TEPs have been used to investigate brain connectivity in several recent studies (Bortoletto *et al* 2015). The use of single pulse TMS coupled with EEG measures of the resulting TEPs was first proposed to measure brain connectivity in work by Ilmoniemi and colleagues (Ilmoniemi *et al* 1997). More recently several authors have proposed using TEPs to measure brain connectivity between a variety of different brain regions including the motor cortex (Bonato *et al* 2006), sensorimotor cortex (Komssi *et al* 2002), and specific Brodmann areas (Rosanova *et al* 2009). For example, TEPs have been used in a study by Nikulin et.al. to investigate how cortical excitability changes when participants begin cued movements (Nikulin *et al* 2003). Specifically, the N100 TEP was reported to decrease as a result of switching from rest to performing a cued movement.

TEPs have also been used to investigate other effects such as the effect of rTMS or cortical inhibition (Casula *et al* 2014), as a neurophysiological indicator of neuropsychiatric disorders (Noda 2020), and to investigate pharmocophysiolgical effects on the brain Darmani and Ziemann (2019).

However, the relationship between TEP-based perturbation measures of effective connectivity and widely used statistical measures of effective connectivity is unclear. TEPs reflect cortical excitability between regions of the brain and can be used to study effective connectivity. However, it is unclear how the information they provide about effective connectivity relates to other widely used metrics of effective connectivity, such as commonly used statistical measures of connectivity.

Additionally, there are several known confounds that arise when generating and measuring TEPs, which can limit their interpretation. TMS produces a very short, loud acoustic noise when activated, which can produce involuntary participant movements and changes in neural activity such as auditory evoked potentials (AEPs) (ter Braack *et al* 2015, Kerwin *et al* 2018). In addition, the TMS coil is placed in close proximity to the scalp and, when activated, can cause vibro-tactile stimulation of the scalp. This can lead to movement artifacts caused by movement of the EEG electrodes, as well as vibrotactile evoked potentials (VTEPs) (Biabani *et al* 2019). TMS can also induce muscle movement artifacts (Hernandez-Pavon *et al* 2022). The TMS can also induce activity within peripheral nerves in the head and neck. This can lead to peripheral nerve evoked potentials (PEPs) in the EEG (Conde *et al* 2019). Finally, brain responses to the TMS depend on the current spontaneous oscillatory brain states (Desideri *et al* 2019, Janssens and Sack 2021) and these brain state dependent responses are known to effect measures of connectivity in the brain Granö *et al* (2022).

Several researchers have suggested methods to first characterise (Bonato *et al* 2006), and then to minimise and remove these confounds, such as masking (Rocchi *et al* 2021), filtering (Biabani *et al* 2019), and the use of de-noising methods such as independent component analysis (ICA) (see Hernandez-Pavon *et al* 2022, Rogasch *et al* 2022for a review). However, these efforts are not always able to remove all confounds and this has even led some researchers to suggest that TEPs are inherently ambiguous (Belardinelli *et al* 2019, Conde *et al* 2019, Siebner *et al* 2019). Indeed, although brain-state dependent responses to TMS may be removed by averaging across repeated trails with careful experiment design, many of the other effects—induced noise in the EEG and evoked potentials (AEPs, VTEPs, and PEPs)—are causally linked to the TMS. Therefore, it is very difficult to differentiate them from TEPs. Various efforts have been made to

develop signal processing pipelines to separate these different effects in the EEG, however they are not able to remove all artifacts and confounds optimally (Rogasch *et al* 2014, Biabani *et al* 2019).

To further explore how TEPs relate to other measures of effective connectivity, while also mitigating the effects of confounds to the TEP, we compare TEP-based measures of connectivity from a motor control visual feedback experiment to established statistical measures of effective connectivity provided by MVAR models from the same experimental dataset. These MVAR-based estimates have been widely used to infer effective connectivity from EEG data (Astolfi *et al* 2007, Cheung *et al* 2010, Haufe *et al* 2010). We expect the TEP-based measures of effective connectivity to be closely related to MVAR-based measures of effective connectivity.

There is a need for careful experimental design to mitigate the effect of confounds on TEP-based measures of effective connectivity. In this study, we use a carefully chosen experimental design to allow us to separate the TEPs from confounding factors. Specifically, we use an experimental design in which delivery of the TMS is kept identical across trials and conditions throughout the study, while the participants are asked to perform different actions or observe different stimuli. Consequently, in this study design any observed significant differences in TEPs between the conditions are likely to relate to changes in effective connectivity that arise from the participant actions or stimuli, rather than noise, spontaneous oscillatory brain state dependent responses to TMS (Desideri *et al* 2019, Janssens and Sack 2021), or other types of confounding factors such as AEPs, VTEPs, PEPs, or TMS-induced noise. Hence, this approach allows us to investigate changes in effective connectivity between conditions.

We use our approach to investigate how TEPs measure effective connectivity between brain regions. Specifically, we measure TEPs under two different conditions during a movement control task. In one condition we provide participants with visual feedback about the strength of their neural activity related to movement control, while in the other condition no feedback is provided. We expect that, in line with results reported by Nikulin *et al* (2003), this will modulate the level of instantaneous effective connectivity between the motor cortex and other areas of the cortex (Noble *et al* 2013), which will in turn be manifested as differences in TEP amplitudes between the two conditions.

2. Methods

2.1. Outline

We make use of a previously recorded joint TMS-EEG dataset to address our research questions. We first investigate TEPs in this dataset to determine whether they differ as a function of visual feedback of movement control. We then identify relationships between TEP- and MVAR-derived measures of effective connectivity by adopting an approach of selecting analysis parameters, e.g. measures of effective connectivity, on an independent subset of the dataset before then applying these selected parameters when processing the remainder of the dataset. This analysis procedure circumvents problems of 'double-dipping', which happen when selection of analysis parameters and data processing are done on the same set of data (Kriegeskorte *et al* 2009).

2.2. Data

We use a previously recorded dataset that was collected for the purpose of evaluating corticospinal excitability during motor control. The results of this study and a detailed description of how the data was recorded are provided elsewhere (Daly *et al* 2018). We describe the key details of this dataset below.

2.2.1. Ethical statement

The data used in this study was originally recorded as part of the work reported in a previous paper (Daly *et al* 2018). In this paper we stated 'ethical approval for the study was granted by the University of Reading research ethics committee, where the research was conducted by the authors, who were based in this institution at the time of the research'.

2.2.2. Participants

A group of 12 healthy adults participated in the study (7 female, 4 left-handed, aged between 21 to 36 years old, with a median age of 25). The participants were each paid £20.00 (GBP) and were screened to ensure they were safe to participate in a joint TMS-EEG experiment following the recommended screening procedures presented by Rossi *et al* (2009).

2.2.3. Experiment

The original experiment was intended to explore how corticospinal excitability differs over the course of a period of movement control and as a result of the presentation of visual feedback to participants. To address these questions participants were asked to sit and, in response to a visual cue, either make movements (repeated flexion and relaxation of all four fingers) with their right hand for a short (5 s) trial or rest for the same length of time. In some trials participants were presented with visual feedback indicating the strength of the event-related desynchronisation (ERD) recorded from their EEG (Stancak and Pfurtscheller 1996), while in other trials they were not given any feedback. TMS was delivered at a range of different time points in the trial. These time points were drawn from a distribution of different possible

time points with many of them determined relative to the strength of the ERD as it changed over time.

The distribution of trials was such that for 90% of the trials participants were asked to move and for 10% of the trials they were asked to rest. For 45% of the trials (half the movement trials) participants were given visual feedback of their ERD strength and for 45% of the trials (the other half of the movement trials) they were not given any feedback. TMS was also delivered in two different ways. For half the trials real TMS was delivered at a pre-identified hotspot location in the brain (as measured by visual inspection of the EMG following the procedure proposed by Rossini *et al* 2015), while for the other half of the trials a sham TMS was delivered by a different TMS coil orientated away from the head and placed at approximately 10 cm distance from the head.

The timing of the TMS was determined by measuring the strength of the ERD recorded via EEG. Specifically, ERD was measured as the percentage decrease in EEG bandpower within the combined alpha and lower beta frequency band (8–20 Hz) relative to the pre-movement cue baseline period via

$$\mathrm{ERD} = \frac{(\mathrm{Base} - \mathrm{ERD})}{\mathrm{Base}} \times 100, \qquad (1)$$

where Base denotes the median EEG bandpower in the 2 s pre-cue baseline period and ERD denotes the EEG bandpower within a 2 s long sliding window that is slid along the 5 s movement period in steps of 0.1 s.

TMS was then delivered at one of the following pseudo-randomly selected time points in each trial: 10%, 20%, 30%, or 40% of ERD strength, or at a fixed time point of 33 ms after the movement cue.

In total we recorded 90 trials with real TMS, 90 sham trials, and 20 rest trials from each participant. Of the real TMS trials 45 were with feedback and 45 without, the same ratio was true for the sham trials. The TMS was delivered at each of the ERD strengths listed above (and the fixed time point of 33 ms) for 36 trials per ERD strength threshold (18 during the real TMS condition and 18 during the sham condition).

The experiment design is described with further details in Daly *et al* (2018). The distribution of trial types and timing of events within a trial is illustrated in figure 1.

2.2.4. TMS

Single pulse monophasic TMS was delivered once per trial at a range of time points in the trial. These time points were determined by online measurement of the ERD strength from participants (see section 2.2.3) and were delivered via a MagStim 200 stimulator (MagStim, USA). The coil used to deliver the TMS was a 10 mm figure 8 coil placed over area M1 of the left motor cortex and orientated at approximately 150°. This coil was stimulated at 120% of the resting motor threshold. Resting motor thresholds were identified for each participant before the start of the experiment following the procedure proposed by Rossini *et al* (2015).

An identical coil positioned 10 cm from the head and orientated away from the head (rotated 180° along the axis of the coil handle) was used to deliver the sham TMS. This sham TMS was delivered with the same strength and timing distribution as the real TMS.

2.2.5. Recording

Both EEG and EMG were recorded from participants. EEG was recorded from 32 electrodes placed using a modified version of the international 10/20 system for electrode placement that clustered the majority of the electrodes over the left motor cortex. Specifically, the following electrodes were used: FP1, FP2, F7, F5, F3, F1, Fz, F4, F8, FC5, FC3, FC1, T7, C5, C3, C1, Cz, C4, T8, CP5, CP3, CP1, CPz, P7, P5, P3, P1, Pz, P4, P8, O1, and O2. The ground electrode was positioned at AFz and the reference electrode at FCz.

A BrainProducts MR TMS compatible EEG amplifier (BrainProducts, Germany) was used to record the EEG at a sampling rate of 500 Hz. This amplifier has previously being shown to record transient TMS artifacts lasting only 10–20 ms in the EEG (Veniero *et al* 2009). Together with appropriate ear protection this recording setup follows recommended good practice to minimise the TMS artifact in the EEG (Mancuso *et al* 2021, Varone *et al* 2021, Farzan and Bortoletto 2022, Hernandez-Pavon *et al* 2023). The impedance's of all the electrodes were kept below 10 kΩ for all participants.

EMG was also recorded from all participants from electrodes placed over the flexor digitorum superficialis muscle. A ground electrode for the EMG was placed on the styloid process of the ulna near the wrist of the right hand. EMG was recorded via a PowerLab data recording system (ADI instruments, USA) at a sampling rate of 4000 Hz.

2.3. Pre-processing

For our study we processed the EEG to remove both physiological and TMS artifacts. We first visually inspected the EEG for artifacts. Specifically, author ID inspected the EEG recorded during each trial, while being blinded to the associated task in the trial, and labelled any artifacts that were identified in the trial. Trials were then rejected if they contained either any visible EMG or movement artifacts on one or more EEG channel (see section 3.1 for the number of removed trials).

Blinks and other eye movement related artifacts were then removed from the EEG via ICA. Specifically, the second-order blind identification implementation of ICA was used to separate EEG within each block into independent components (Belouchrani *et al* 1993). These components were

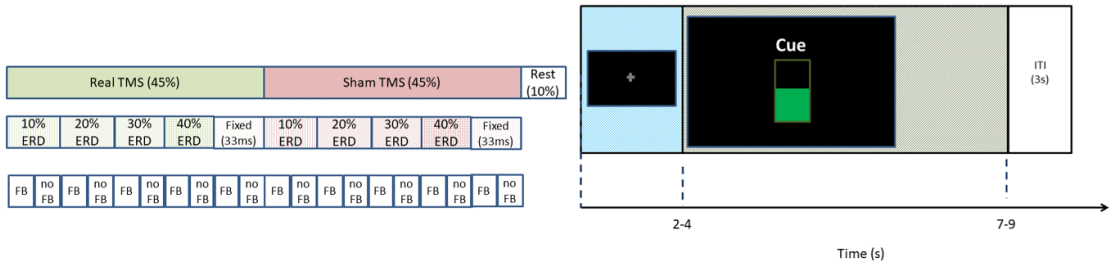

Figure 1. The distribution of trial types within the experiment (left; note the trials were presented in random order to participants) and the timing of events within a single trial (right).

then inspected by author ID in the time, frequency, and spatial domains, and components containing blinks or other eye movement related artifacts were removed before reconstruction of the cleaned EEG. Note, it was not necessary to interpolate any individual channels in our dataset because we did not need to remove any channels from the data for any participants.

Slow drift artifacts were then removed from the EEG via subtraction of a fitted polynomial function. Specifically, a second order polynomial was estimated for each trial of EEG and then subtracted from the trial in order to remove slow drifts and baseline shifts in the EEG.

The TMS artifact was removed from the trials via a process of piece-wise cubic interpolation. Specifically, following the approach proposed in Conde *et al* (2019), EEG within a 16 ms time window −0.002 to 0.014 s relative to the time of the TMS delivery was replaced with a piece-wise cubic interpolation estimated from the EEG in the remainder of the trial.

The data was then further pre-processed slightly differently for the TEPs and the MVAR models.

2.3.1. TEP pre-processing

The EEG was segmented into a set of trials for which real TMS was delivered in order to characterise the TEPs. These trials are denoted T^{TEP}.

Additionally, a second subset of trials for characterising the TEPs during the sham condition were extracted from the EEG. This sham subset of trials (denoted T^{SHAM}) was used to verify that any observed TEPs were the result of TMS and not potential confounds caused by interactions between the visual and auditory systems as a result of feedback presentation (see section 2.9).

We hypothesise that TEPs (which occur after delivery of TMS) reflect the effective connectivity within the brain at the time point when TMS is delivered to the brain. Therefore, TEP-based measures of effective connectivity are most likely to reflect the instantaneous effective connectivity at that time point.

The trials which are used to characterise the TEPs (T^{TEP} and T^{SHAM}) are defined as the epoch of EEG from −2.0 s to 2.5 s relative to the time point at which the TMS was delivered to the participants.

A 20th order notch filter at 50 Hz was applied to both the T^{TEP} and T^{SHAM} trials in order to first remove 50 Hz power-line noise. This was followed by a 4th order low-pass filter, which was used to filter the T^{TEP} and T^{SHAM} trials to a frequency range below 100 Hz.

The T^{TEP} and T^{SHAM} trials were than baseline corrected by subtracting the median amplitude of the EEG on each channel from the pre-TMS baseline period (−2 to −0.002 s relative to the TMS time point) from the remainder of the EEG in the trial.

2.3.2. MVAR pre-processing

The EEG was also separately processed and segmented into a set of trials for extracting MVAR parameters. First, the unsegmented EEG was *z*-scored across channels following recommendations by Ding *et al* (2000) to set the variance of each channel to the same amount in preparation for later fitting of an MVAR model to the data (see section 2.5).

The set of *z*-scored EEG was then segmented into a set of trials, denoted T^{conn}, which were used to fit the MVAR models.

MVAR-based estimates of effective connectivity measure connectivity within an epoch of EEG that needs to be of sufficient length to estimate the MVAR parameters. Furthermore, this time window cannot include the time at which TMS is delivered as the TMS artifact in the EEG (or the interpolated EEG used to replace it, see above) will bias the MVAR parameter estimation. Therefore, to estimate effective connectivity at approximately the same time point via MVAR models as the TEP based measures, a slightly different time window is needed for the T^{conn} trials.

The T^{conn} trials were defined as the epoch of EEG from −0.5 s to 0.2 s relative to the TMS time point. After processing these trials the MVAR model parameters are then estimated from the 0.5 s EEG epoch immediately before the TMS delivery (−0.5 s–0 s). Note, a longer time window is needed to estimated TEPs because of the need for baseline correction,

Table 1. Trial set types.

Trial type	Description
T^{TEP}	Trials containing real TMS events used for estimating TEPs
T^{SHAM}	Trials containing sham TMS events used for estimating TEPs
T^{MVAR}	Trials containing real TMS events used for estimating MVAR parameters.

while the MVAR trials include 0.2 s after the TMS artifact to allow accurate removal of this artifact before focusing on the time window up to the TMS delivery time.

The T^{conn} trials were not narrow-band filtered in order to fulfil the model assumption that the MVAR coefficients transform white Gaussian noise into the observed data (Schlögl, A. (personal communication)). When the MVAR model is fit to narrow-band data, the noise term is also narrow-band, i.e. it is not white, which in turn produces inaccuracies in the estimated MVAR coefficients.

Following recommendations from Ding *et al* (2000), and as used in Williams *et al* (2018), the T^{conn} trials were also z-scored across trials to remove ERP components from the EEG prior to fitting the MVAR models (see section 2.5).

2.3.3. Pre-processed trials

In summary, we extract three sets of trials from the EEG. These are summarised in table 1.

All three types of trial were re-referenced to a common average reference montage.

2.4. TEP measurement

The TEPs were characterised from the pre-processed T^{TEP} trials by inspecting the grand average TEPs of the trials on each channel under each of the feedback conditions (with ERD feedback and without ERD feedback provided to participants).

Based upon our inspection of the TEP grand averages we then identify time points of key TEPs. These time points are reported in section 3. The mean amplitude of the TEP at these time points on each channel within each trial are then extracted and used to measure effective connectivity between the location of the TMS coil and all other EEG channels.

We measure the differences in mean TEP amplitudes within these time points between the feedback and no feedback conditions to determine if the provision of visual feedback to participants influences effective connectivity. We hypothesise that providing visual feedback to participants about their ERD strength as they perform a movement task will influence effective connectivity between the motor cortex and other brain regions. As TMS was delivered to the left motor cortex in our experiments we expect that TEPs will allow us to measure effective connectivity between this brain region and other brain regions at which EEG electrodes are placed.

2.5. MVAR measurement

To measure effective connectivity using statistical analysis of the EEG, MVAR models were fitted to the EEG in the T^{conn} trials.

For a given set of measurements of neural activity $S(t)$ at time $t, \in [1, \ldots, T]$ (where T denotes the length of the T^{conn} trial), the MVAR model is defined as

$$S(t) = \sum_{k=1}^{p} A(k)\, S(t-k) + E(t). \tag{2}$$

according to which the current value of S is expressed as the sum of a linear weighted combination of the past values of S up to a given model order p, and white Gaussian noise E. $A(k)$ denotes an $M \times M$ matrix that contains the model coefficients at lag k, defined as

$$A(k) = \begin{bmatrix} A_{11}(k) & \cdots & A_{1M}(k) \\ \vdots & \ddots & \vdots \\ A_{M1}(k) & \cdots & A_{MM}(k) \end{bmatrix}, \tag{3}$$

where M is the number of EEG channels. The coefficient $A_{i,j}(k)$ denotes the linear weight relating $S_j(t-k)$ to $S_i(t)$ at lag k, thus furnishing a measure of causal influence from channel j to channel i at lag k. In our analysis, we identified the model order p via the Bayesian information criterion (BIC) (Nicolaou and Georgiou 2013) from the training data.

We use the MVAR model to extract the following measures of effective connectivity from the EEG.

(i) Directed coherence
(ii) Directed transfer function
(iii) Partial directed coherence
(iv) Generalised partial directed coherence
(v) Coherence
(vi) Partial coherence

Directed coherence is a bivariate, frequency-specific measure of effective connectivity while Partial directed coherence is a multivariate extension of Directed coherence (Baccala and Sameshima 2001). Generalised partial directed coherence adjusts the partial directed coherence measure for severe imbalances in the variance of innovations (Baccala *et al* 2007). Finally, the Directed transfer function is a multivariate measure of information flow between sources (Kaminski and Blinowska 2014). These measures can be derived from the MVAR parameters.

2.6. TMS coil estimation

While recording our dataset we used a wall mounted clamp to hold the TMS coil in place, with manual guidance of the coil location and without the use of neuronavigation to adjust to participant head movement during the experiment. This means we do not

have a completely accurate recording of the location for the TMS coil relative to the EEG channels.

To more accurately estimate of the TMS coil location we used a source localisation method (Grech *et al* 2008). Specifically, we use a finite element model of the head (generated from an averaged anatomical MRI available from the SPM toolbox) (Awada *et al* 1997, Hallez *et al* 2007, Wolters *et al* 2007). We split this MRI into 3 elements (scalp, skull, and brain), and specified conductivity of each layer using the following standardised values: brain = 0.75 $s\,m^{-1}$, skull = 0.0042 $s\,m^{-1}$, and scalp = 0.33 $s\,m^{-1}$. These values were chosen based on recommendations in Geddes and Baker (1967), Baumann *et al* (1997), Hallez *et al* (2007). Note, most modern source localisation methods will seek to further segment the brain into cortical spinal fluid, white matter, and gray matter (Hallez *et al* 2007), but as the source we are interested in (the TMS coil) is outside the head we do not need such a precise model for our purposes. We used dipole fitting to estimate the mean location over participants and trials of the dipole related to the TMS. We used methods from the Fieldtrip toolbox (version 20190819 (Oostenveld *et al* 2011)) in Matlab (version 2019a).

2.7. Parameter search

Each of the MVAR-derived estimates of effective connectivity is extracted from a single frequency band of width 1 Hz. Specifically, the 6 different MVAR-based estimates of effective connectivity described in section 2.5 were extracted from frequency bands from 1 to 50 Hz. This resulted in a set of 6 different MVAR-derived estimates of effective connectivity in 50 different frequency bands, giving a set of 300 candidate MVAR estimates of effective connectivity.

MVAR-based estimates of effective connectivity provide an estimate of the connectivity between all available pairs of channels. However, TEP-based perturbation measures of connectivity can only provide a measure of the connectivity between the subset of channels positioned directly underneath the TMS coil and all other channels. Therefore, to meaningfully compare MVAR-based estimates of connectivity with TEP-based measures of connectivity it is necessary to just extract the subset of MVAR-based estimates of effective connectivity between the subsets of channels in the neighbourhood of the TMS coil and all other EEG channels. This subset of connectivity values is then compared to the TEP-based measure of effective connectivity.

In order to identify the optimal set of parameters we randomly divided our dataset of 12 participants into subsets using a 2×2 cross-fold train and test scheme. The resulting training and a testing sets each contained 6 participants. We then use the training set to identify which combination of MVAR-based estimates of effective connectivity and analysis parameters most closely reflects the TEP-based measure of effective connectivity, before verifying this measure in the held-out test set.

It is first necessary to identify the subset of EEG channels closest to the site of the TMS coil. Within the training set we first estimated the location of the TMS coil via source localisation (see section 2.6). Within this same training set we then search for the subset of channels that most accurately captures EEG activity from the region of the brain directly stimulated by TMS.

To do this we search for a subset of channels located near the estimated position of the TMS coil by progressively adding EEG channels to the set of channels in the neighbourhood of the TMS coil in order of increasing Euclidean distance from the estimated location of the coil.

We then performed an exhaustive parameter search to identify which combination of these parameters (number of proximal EEG channels, frequency band of interest, and candidate MVAR-derived statistical estimates of effective connectivity) most accurately reflects the perturbation based measure of effective connectivity provided by the TEPs.

Within the training set we analysed the differences in effective connectivity patterns between the feedback and no feedback conditions on a per participant basis for the TEP-based measure of connectivity and for each of the candidate MVAR-based estimates of connectivity over each of our search parameters. For a given set of parameter values we measure the difference in connectivity patterns between the feedback condition and the no feedback condition via Bhattacharyya distance (a measure of the statistical similarity between two distributions (Theodoridis and Koutroumbas 2006)).

Thus, for each participant and each measure of connectivity (TEP or MVAR) we form relative adjacency matrices that indicate the differences in connectivity—between the feedback vs. no feedback conditions—between the EEG channels located in the neighbourhood of the TMS coil and all other EEG channels. This is defined as $C_{i,j} = \{x \in \mathbb{R}\,[0 \leqslant x \leqslant 1]\}$ where i indicates the EEG channel in the neighbourhood of the TMS coil and j indicates one of the other EEG channels.

The set of TEP-based adjacency matrices is denoted C^{T} and the set of MVAR-based adjacency matrices is denoted C^{M}. These adjacency matrices denote the topology of connectivity over the head. For each participant, we determine if this topology is similar between TEP and MVAR measures by measuring the Pearson's correlation coefficients between the topographic maps of connectivity (Wang *et al* 2004). This provides a measure of how similar the connectivity patterns are between the TEP and MVAR measures. The parameter set that results in

an MVAR-based estimate of connectivity that is most similar to the TEP based measure of connectivity over all participants in the training set is then chosen and evaluated within the held out test set.

2.8. Statistics

To verify that the MVAR-based estimate of effective connectivity with the selected parameter set is more similar to the TEP-based measure of effective connectivity than could have occurred by chance, a bootstrapping significance test is adopted. In the test set, the pattern of distances between EEG channels in the neighbourhood of the TMS coil and all EEG channels, are measured for each participant by both the TEP-based measure of connectivity and the MVAR-based estimate of connectivity. The distance between the network topologies over the scalp of these two connectivity estimates is then measured via Pearson's correlation coefficient.

A null distribution is then generated by generating a new null connectivity matrix C^{b} of the same dimensions as the matrix C^{M} but with edge weights randomly drawn from the range 0 to 1. The correlation between C^{T} and C^{b} is then measured over 4000 re-generations of C^{b} to estimate the null distribution. The probability that the measured correlation between C^{T} and C^{M} was drawn from this distribution is then estimated in order to evaluate the significance of the measured correlation between C^{T} and C^{M} in the test set.

2.9. Confounds

TEPs arise from magnetic stimulation of one brain region by TMS. However, the TMS device is also capable of producing other effects in the EEG that need to be considered as possible confounds when performing analysis of the TEP (Conde *et al* 2019).

The TMS device produces a loud, short duration, acoustic click noise when activated. This acoustic effect can result in AEPs, which are time locked to TMS activation and, therefore, can be very difficult to differentiate from TEPs. Furthermore, these acoustic effects can differ between real TMS and a sham condition due to conduction through the bone as a result of direct contact between the coil used to deliver real TMS and the scalp. TMS also produces vibro-tactile stimulation of the scalp when stimulated and peripheral nerve stimulation of nerve fibres in the scalp. Both these forms of stimulation can produce evoked potentials that also act as confounds in the analysis of the TEP (Conde *et al* 2019).

Our experimental design mitigates these known confounds of the TEP by investigating how TEPs are effected by visual feedback to the participant. In both trial conditions in our experiment (feedback and no feedback) the TMS is delivered at the same location on the head and with the same timing and amount of power. Thus, AEPs, bone conduction, vibro-tactile ERPs, and peripheral nerve stimulation ERPs are unlikely to be significantly different between the feedback and no feedback conditions, mitigating these potential confounds.

However, presentation of visual feedback to participants may act to effect auditory evoked potentials (AEPs) through modulation of acoustic attention networks (Braga *et al* 2016). Put another way, changes in visual stimuli can act to modulate participants acoustic attention, which may in turn effect AEP amplitudes.

To investigate this potential confound we also repeat our analysis of the TEPs with the sham TMS condition. Sham TMS produces approximately the same amount of acoustic noise as real TMS (the sham coil was only approximately 10 cm away from the real coil and activated with the same level of power). We hypothesis that, if the visual feedback to the participants is significantly modulating AEPs, there should also be significant differences in evoked potentials between the feedback and no feedback conditions during the sham trials. On the other hand, if there is no AEP confound in the TEPs there should not be a significant difference in evoked potentials between the feedback and no feedback conditions during the sham TMS trials.

3. Results

3.1. Pre-processing

A mean of 4 trials ($\pm$3.19 standard deviation) were removed from each participant due to excessive artifacts. ICA was used to remove physiological artifact components during the pre-processing stage. This resulted in an average of 1.98 ($\pm$1.44 standard deviation) ICs being removed from each participants data.

3.2. TMS coil location

The mean location of the TMS coil, estimated via source localisation, is illustrated in figure 2.

It is not possible to verify the location of the coil numerically as we did not record the exact location of the TMS coil while recording the data. However, as TMS was applied over the left motor cortex the estimated location of the coil appears to be approximately correct.

3.3. TEPs

TEPs are characterised at each EEG channel location on the head for each of the two conditions, visual feedback and no visual feedback. Figure 3 illustrates the TEPs at all channels on the head.

The TMS coil is located approximately over the centre of the left motor cortex (area M1 of the left motor cortex) and some TEPs are present over this

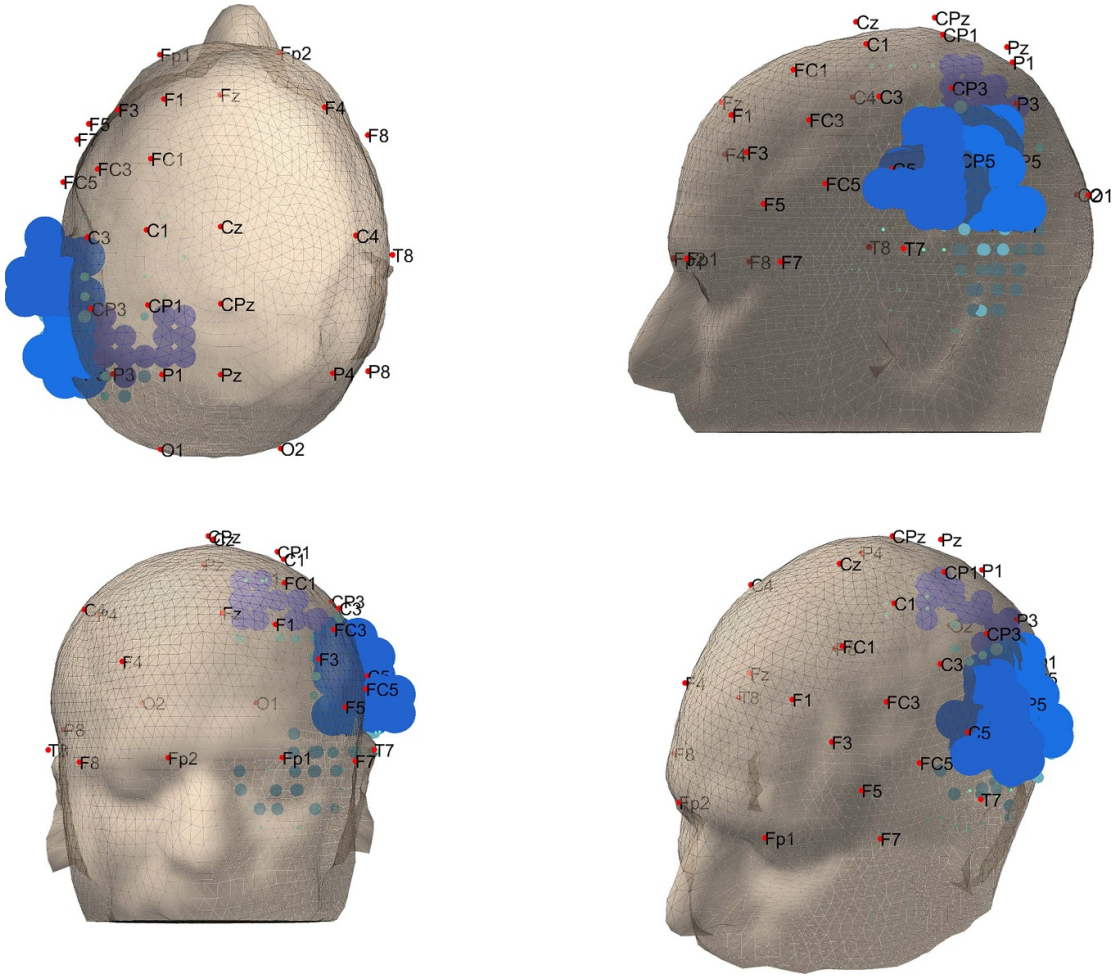

Figure 2. Heatmap of estimated locations of the TMS coil. The location of the coil is illustrated in shades of blue with the size and colour intensity indicating the approximate number of times the paddle was estiamted to be in a particular location. The red dots illustrate the locations of the EEG channels.

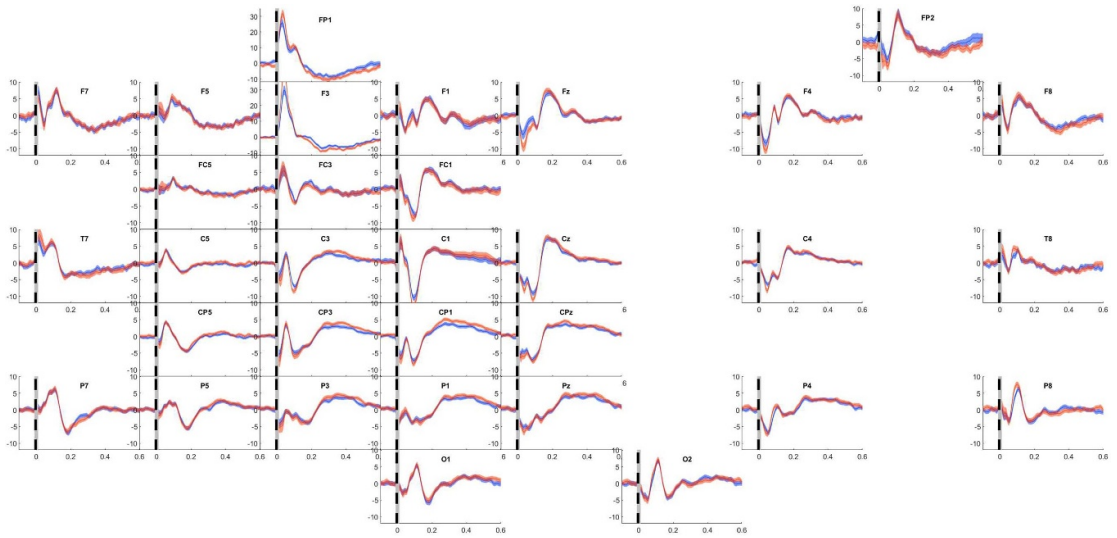

Figure 3. Grand average TMS evoked potentials (TEPs) from all participants over all EEG channels for the two conditions, visual feedback given to participants (blue) and no feedback given to participants (red). The dark lines represent the mean average amplitudes of the TEPs, while the shaded areas represent the 95% confidence intervals.

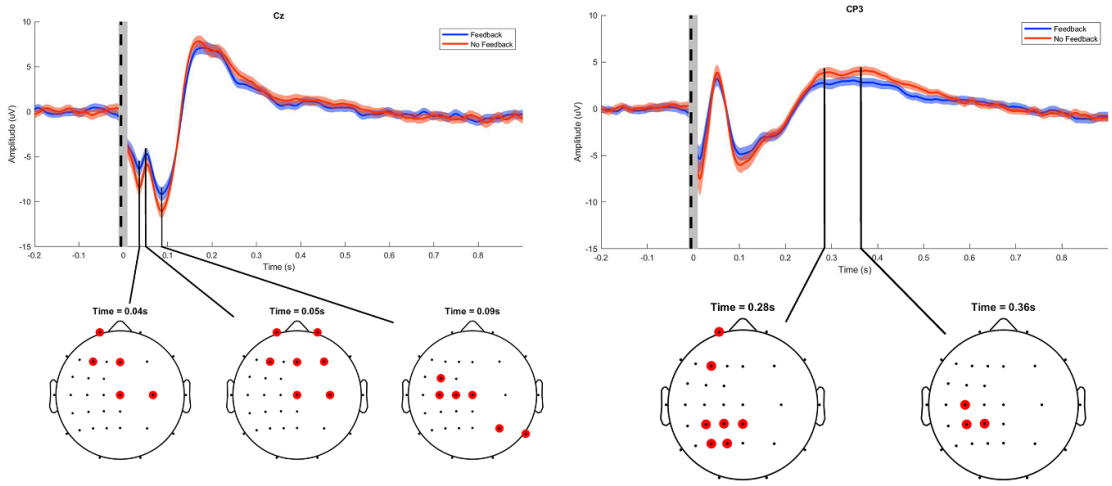

Figure 4. Examples of grand average TEPs from all participants on EEG channels Cz and CP3 for the two conditions, visual feedback given to participants (blue time series) and no feedback given to participants (red time series). The dark lines represent the mean average amplitudes of the TEPs, while the shaded areas represent the 95% confidence intervals. The topographic plots illustrate channels at which significant differences are found (red locations, $p < 0.05$, t-test, corrected for multiple comparisons via false discovery rate correction).

region of the brain. There are also TEPs at several other locations in the brain including both the left and right prefrontal cortex and the occipital cortex. Furthermore, there are marked differences in the amplitudes of the TEPs between the feedback vs. no feedback conditions on several channels. This suggests that the presentation of visual feedback to participants during a motor control task effects the level of effective connectivity.

This can be observed in detail by inspecting the TEPs on individual channels. Channels Cz and CP3 are selected as interesting examples of the TEPs evoked during our experiment. These channels are illustrated in figure 4.

There are TEPs present at a range of time points with clear N40, P50, N90, P280, and P360 TEPs on many channels. Clear TEPs may be observed under both conditions, with negative peaks at approximately 40 ms, and 90 ms, as well as positive peaks at 50 ms, 280 ms, and 360 ms. There are also clear differences in the TEP amplitudes between the two conditions. On channels located over the central cortex, such as Cz, these differences are most prominent from approximately 40 ms to 90 ms after the TMS is delivered to the participant. A detailed illustration of how these TEPs at 90 ms differ between conditions over all channels is illustrated in figure 5.

On channels located over the left central-parietal cortex, such as CP3, the significant differences between the feedback and no feedback conditions are considerably later and peak at times of 280 ms and 360 ms. This suggests that the effective connectivity between the site of the TMS (approximately over area M1 of the left motor cortex) and multiple brain regions differs as a function of visual feedback of the ERD strength to participants and results in changes to both early and late TEPs.

We also investigated the possibility that interactions between the change of visual stimuli (between the feedback and no feedback conditions) and attention networks were producing confounding AEPs. Specifically, we repeated our analysis with the sham TMS condition. If there is an AEP confound effect we would expect to see a similar pattern of significant evoked potentials in the sham TMS condition compared to the real TMS condition.

After correction for multiple comparisons we did not find any significant differences in evoked potentials between the feedback and no feedback conditions during the sham TMS trials. This is illustrated in figure 6, which shows an example of the TEPs produced during the sham condition along with the topographic significance maps for the same time points we previously identified during the real TMS condition. There are no significant differences observed between the feedback and no feedback conditions at any time points or channels during the sham TMS condition.

3.4. Connectivity measures

We investigate how MVAR-based measures of connectivity compare to TEP-based measures of connectivity. Within the training set, the BIC was used to identify the optimal model order for the MVAR model from the training set. This revealed that over the 4 folds within our 2×2 cross-fold validation scheme, a model order of 4 was optimal for fitting MVAR models to our dataset. Additionally, our parameter search within the training set revealed that the set of EEG channels that are in the neighbourhood of the TMS coil consists of channels FC3, C5, C3, and CP3. Channels C3 and C5 are selected in all folds, while channels FC3 and CP3 are selected in 2 folds.

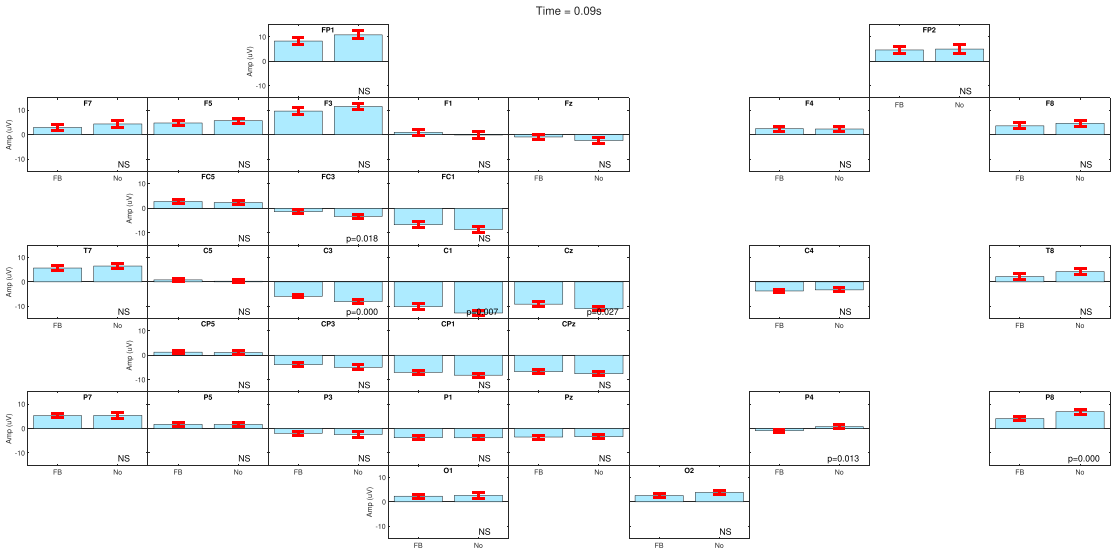

Figure 5. The mean and confidence intervals of the TEP amplitudes at 90 ms for the feedback (FB) and no feedback (No) conditions over all channels and participants. Significant differences are indicated via '*p*' values (*t*-test, corrected for multiple comparisons via false discovery rate correction), while non-significant differences are indicated via 'n.s'.

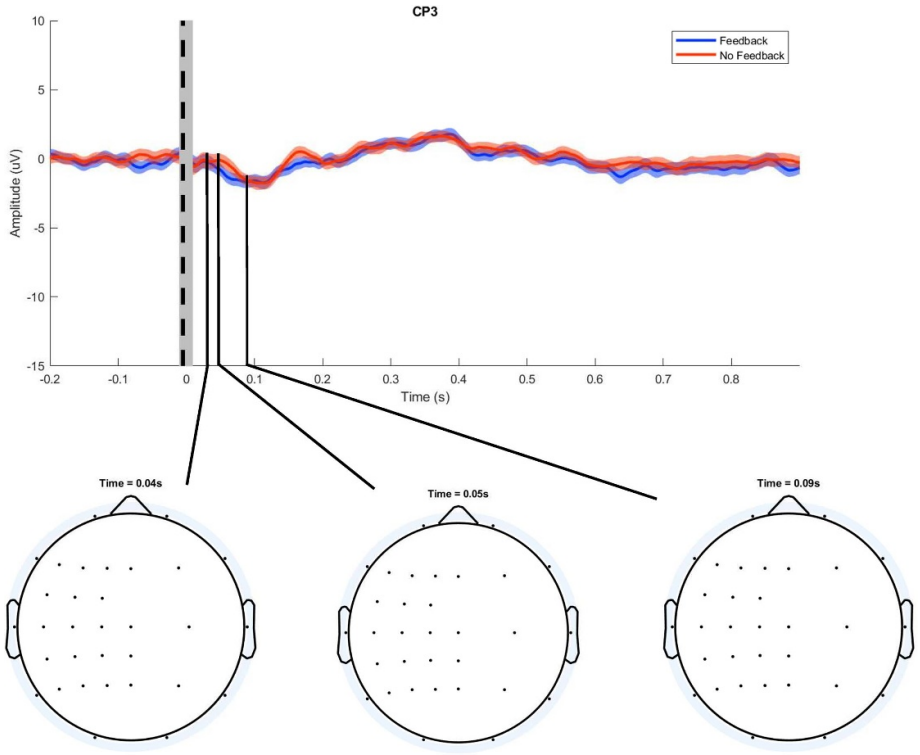

Figure 6. Grand average TEPs from all participants over example EEG channel CP3 for the two conditions, visual feedback given to participants (blue time series) and no feedback given to participants (red time series) during the sham TMS condition. The dark lines represent the mean average amplitudes of the TEPs, while the shaded areas represent the 95% confidence intervals. The topographic plots indicate channels at which significant difference are found (note, no significant differences are observed during the sham condition).

The MVAR-based estimates of connectivity across the available frequency bands are compared to the TEP-based connectivity maps derived from the N40, P50, N90, P280, and P360 TEPs within the training set. For each of these evoked potentials we systematically search for MVAR parameters which result in connectivity patterns that are similar to the TEP-based connectivity patterns (as measured by Pearson correlation coefficient). We then validate these identified MVAR patterns in our held out test set.

Our results reveal that the N40 TEP is most similar to the MVAR-derived measures of effective connectivity, based on coherence, at 39 Hz ($\pm$7.32 Hz over folds). Specifically, partial squared coherence is

Table 2. MVAR parameters selected over folds.

Fold	Causality measure	Frequency (Hz)
1	Partial coherence	43
2	Partial squared coherence	35
3	Generalised directed partial coherence	46
4	Partial squared coherence	30

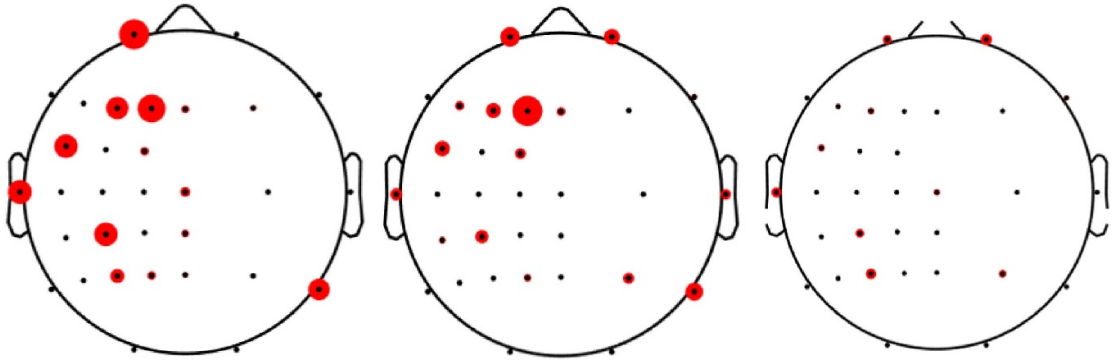

Figure 7. Topographic maps—over EEG channels—of Bhattacharyya distances between the feedback and no feedback conditions. The left plot indicates Bhattacharyya distances between feedback and no feedback in N40 TEP amplitudes in the training set, while the centre plot indicates Bhattacharyya distances between feedback and no feedback in directed coherence at 30 Hz (derived via the MVAR model) in the training set. The radius of the red highlighted circles indicate the Bhattacharyya distances comparing the feedback vs no feedback conditions. The right plot illustrates the differences between the TEP and MVAR measures of connectivity.

identified, from the training set, in 2 folds, partial coherence in 1 fold, and generalised directed partial coherence in 1 fold, as producing the connectivity pattern that is most similar to the TEP connectivity pattern in the test set. These findings are summarised in table 2. We further verify this is statistically significant in the test set via a bootstrapping approach. This reveals that the patterns of effective connectivity identified by directed coherence and TEPs are statistically significantly similar to one another in the testing set (correlation coefficient $r = 0.282$, $p < 0.001$).

The similarity of the TEP and MVAR connectivity patterns in the training set are illustrated in figure 7, while figure 8 illustrates the results in the testing set. These results suggest that directed coherence in the frequency range 30–46 Hz measures effective connectivity in a way that is most similar to the way effective connectivity is measured by the perturbation based measure provided by TEPs.

In summary, it can be seen that EEG electrodes over the left pre-frontal cortex and EEG electrodes over the central cortex differ significantly in effective connectivity strength with channels in the neighbourhood of the TMS coil between the feedback and no feedback conditions. Similar connectivity patterns are found via TEPs and in directed coherence at 30–46 Hz.

4. Discussion

In this paper, we investigated how TEPs can be used to measure effective connectivity. TEPs have been described as a source of ambiguity in studying brain connectivity (Belardinelli *et al* 2019, Conde *et al* 2019, Siebner *et al* 2019) due to the difficulties in disentangling the TEP from the multitude of potential confounds caused by the TMS. However, our experimental design allows us to mitigate many of these confounds by exploring how TEPs change as a result of visual stimuli. We also make use of a sham TMS condition to account for any additional potential confounds arising from interactions between visual stimuli and auditory attention networks (Braga *et al* 2016).

Our results reveal a significant difference in TEP amplitudes between the visual feedback and no feedback conditions when participants attempt motor control of the right hand. This difference is observed between the M1 region of the motor cortex and both the prefrontal and central cortex, with significantly higher amplitude TEPs observed in the no feedback condition, suggesting increased effective connectivity from the motor cortex to multiple other cortical areas when no visual feedback is presented. We observed several TEP components including negative components at between 0.04–0.09 s and later positive components at between 0.28 s to approximately 0.4 s. The early negative components are similar to the N100 TEP, which has been previously reported to be effected by performing cued movements (Nikulin *et al* 2003).

These findings suggest that effective connectivity (as measured by TEPs) changes dynamically during motor execution. Furthermore, these changes in the

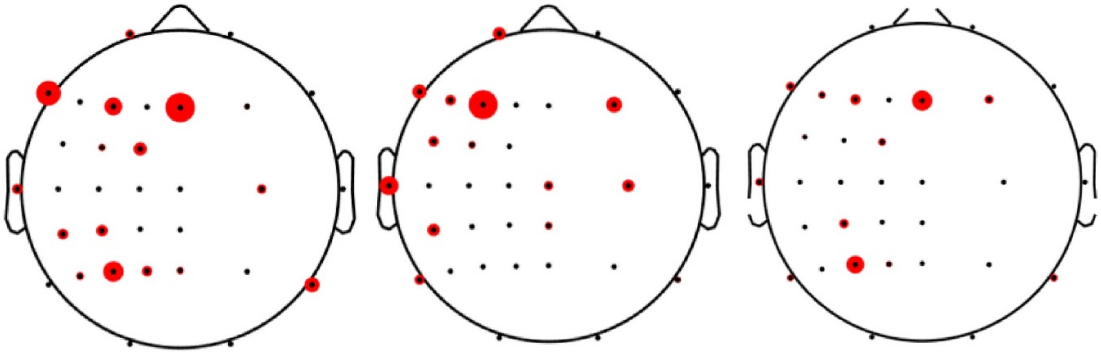

Figure 8. Topographic maps—over EEG channels—of Bhattacharyya distances between the feedback and no feedback conditions. The left plot indicates Bhattacharyya distances between feedback and no feedback in N40 TEP amplitudes in the testing set, while the centre plot indicates Bhattacharyya distances between feedback and no feedback in directed coherence at 30 Hz (derived via the MVAR model) in the testing set. The radius of the red highlighted circles indicate the Bhattacharyya distances comparing the feedback vs no feedback conditions. The right plot illustrates the differences between the TEP and MVAR measures of connectivity.

dynamics of effective connectivity are modulated by the provision of visual feedback of the ERD to participants. This further supports the notion that effective connectivity should be considered as a dynamic process, rather than a static fixed state.

Our results are supported by findings from previous studies that report significant connectivity between M1 and the SMA during both motor planning and movement control (Yeom *et al* 2020). For example, Nikulin et.al. reported that the N100 TEP decreased as a result of switching from rest to a cued movement (Nikulin *et al* 2003) and we see a significant change in N100 amplitude a result of switching from feedback to no feedback during a cued movement. Our results are also supported by a recent fMRI study, which shows that connectivity between the premotor cortex and the putamen is modulated by visual feedback to the participant during movement control (Noble *et al* 2013). Given this corroboration from previous studies, our results show how TEPs can be used to measure changes in effective connectivity as a result of visual feedback of motor control.

While TEPs have been previously proposed by a number of authors as a measure of effective brain connectivity (Ilmoniemi *et al* 1997, Hampson and Hoffman 2010, Rogasch and Fitzgerald 2013, Vink *et al* 2017) others have raised concerns about the influence of confounds on interpretation of the TEPs (Biabani *et al* 2019, Conde *et al* 2019, Siebner *et al* 2019, Freedberg *et al* 2020, Rocchi *et al* 2021). These confounds include a number of evoked potentials that arise directly from delivery of the TMS. Consequently, they have proved challenging to separate from the TEP and even lead some to conclude the TEPs are inherently ambiguous (Belardinelli *et al* 2019, Conde *et al* 2019, Siebner *et al* 2019).

Our study mitigates the effects of many of these confounds on the TEP. By asking participants to engage in some specific task we can use TEPs to measure task-related changes in effective connectivity between brain regions. Specifically, factors that are likely to confound the TEP are controlled between conditions. For example, the acoustic noise of the TMS is constant between conditions, as is the vibro-tactile stimulation resulting from the TMS, and induced electrical artifacts. Additionally, the orientation of the TMS coil could produce changes in field strength from trial to trial and this is known to effect EEG responses to TMS (Casarotto *et al* 2010). Indeed, as in our study, the coil was hand-held and no neuronavigation system was used coil orientation is likely to change randomly from trial to trial. However, as the content of the trials (feedback vs no feedback) was randomly ordered and unpredictable to both the participant and experimenter (who was holding the coil) this is unlikely to differ systematically between the feedback and no feedback conditions and hence unlikely to confound the TEPs.

Consequently, our results support our hypothesis that TEPs differ significantly between study conditions in a way that could not have been caused by many types of TMS-related confound. Additionally, the confound that arises from interaction between visual stimuli and auditory attention is controlled for by use of a sham condition. However, it is important to note that vibro-tactile stimuli may also induce some changes in acoustic stimulation and that this cannot be controlled by the use of our sham condition as our sham TMS is too far from the head to induce vibro-tactile stimulation. Further investigation of this potential confound is required.

It may be argued that the presentation of visual feedback to participants is likely to produce a visual evoked potential (VEP) and that this VEP will differ between the feedback vs. no feedback conditions. However, the timing of the delivery of our TMS is not determined by, or temporally linked to, the presentation of visual feedback. Meaning that any VEPs that arise from the presentation of visual feedback are not synchronised over trials with the TMS and, consequently, these VEPs will cancel out when averaged across multiple trials. This can be further verified by inspecting the ERPs in the sham condition. The sham condition contains identical visual feedback, delivered in an identical manner at times that are unpredictable to participants (pseudo-randomised across trials). Thus, if our observed TEPs contain VEP elements we would expect these to remain in the sham condition. However, there are no apparent VEPs in the sham condition, further verifying that VEPs are not influencing our TEPs.

There are several additional types of artefact that can arise in the EEG as a result of TMS and hence confound the TEP. These artefact types are detailed by Varone *et al* (2021) and, in addition to the artifacts we have already considered above (pulse artifacts, evoked potentials, movement artifacts etc) they include slow capacitive discharge in EEG electrodes, movement of the electrodes, polarisation of the elections, and recharge artifacts. We followed recommendations in Varone *et al* (2021) to remove these artifacts through use of low impedance EEG recordings, the use of Ag/AgCl electrodes, aligning the EEG wires orthogonally to the coil handle, the use of a direct-coupled amplifier, earplugs for participants, and by timing the recharge of the TMS device to occur in between trials.

In addition to these measures several researchers recommend the use of relatively high EEG sample rates to aid interpolation-based removal of the pulse artifact and accurate reconstruction of the TEP. However, a high sampling rate is just one method, among many, that can be used to reduce the effect of TMS artifacts and enable their effective removal. For example, Farzan and Bortoletto (2022) note that specialised amplifiers (such as the one used in our study) or electrodes can be used instead of high sample rates to support effective interpolation to remove the TMS artifact, while Varone *et al* (2021) note that instead of relying exclusively on high sample rates a number of recording circuits, such as sample and hold circuits, have been proposed to minimise the effect of the TMS artifact. Indeed, several TEP studies have shown that sample rates of 500 Hz or less can allow effective removal of the TMS artifact and characterisation of the TEP (Thut *et al* 2005, Yamanaka *et al* 2013, Sasaki *et al* 2021).

To further investigate TEPs as measures of effective connectivity, we sought to verify if an established statistical estimate of effective connectivity relates to the perturbation-based measures of effective connectivity provided by TEPs. To do this we used MVAR models to estimate effective connectivity between EEG channels in the neighbourhood of the TMS coil, and all EEG channels. We extracted 4 different measures of effective connectivity at 50 different frequency bands and split our data into training and testing sets to first search for the statistical estimate of effective connectivity that most closely matched the perturbation measure of effective connectivity identified by TEPs and then verify it in the held out test set.

Our results revealed that directed coherence between 30–46 Hz is most similar to the effective connectivity measure provided by the early N40 TEP. The 30–46 Hz frequency is within the upper beta frequency band, which is widely reported to be involved in motor planning and control (Chung *et al* 2017). These results are similar to those reported in a recent study (Vink *et al* 2019) which demonstrates a correspondence between TEPs and some measures of functional connectivity. However, our study is the first one to our knowledge demonstrating a correspondence between TEP-based and statistical measures of effective connectivity. Aside from giving insight into the nature of the relationship between TEP-based and statistical measures of effective connectivity, our finding provides further support for the use of TEPs to measure changes in effective connectivity as a result of visual feedback of motor control.

However, our results must be interpreted with caution. Specifically, our MVAR parameters and our TEP amplitudes are, by necessity, measured from slightly different time windows. MVAR parameters are estimated from the 0.5 s window immediately before the TMS, while TEP based connectivity provides a measure of cortical excitability between brain regions and is measured at the time point of the TMS. It is possible that effective connectivity patterns are relatively stable over this short time period. However, it is also possible that, during the course of movement control, instantaneous connectivity patterns are changing relatively rapidly and the different methods are not able to capture this change in connectivity dynamics perfectly. Further investigation is required.

Additionally, the relatively small dataset of 12 participants used in our study prevents us from drawing further conclusions from our results. We took measures to guard against false positives, such as FDR-based correction for multiple comparisons (Benjamini and Hochberg 1995), when assessing TEPs and using low p-value thresholds of $p < 0.001$ when comparing MVAR-based and TEP-based connection patterns. Applying FDR-based correction was, for example, shown to be effective in not allowing any (false positive) statistically significant differences

in TEP amplitudes between the feedback and no-feedback trials, in the sham TMS condition. However, we acknowledge the risk of false positive and false negative findings due to the low small sample size. Specifically, the small sample size might be reflected in exaggerated statistically significant effects (false positives) or in missing statistically significant effects due to the low statistical power (false negatives) (Button *et al* 2013). Further, we note that we used a valid and recommended approach to select the optimal set of parameters (Kriegeskorte *et al* 2009) for a given analyses, which promotes the robustness of our conclusions. To provide additional evidence of the robustness of our approach we report the parameters found via our approach over the different folds within our study population. We found only small differences in parameters identified over each fold.

Additionally, the set of 32 EEG channels that we recorded from are biased to the left hemisphere. This is a result of the specific question that the prior study (from which our dataset is taken) was attempting to address. However, it means that we have far fewer electrodes available over the right hemisphere than the left hemisphere. Consequently, connectivity patterns—identified via both TEPs and MVAR models—that involve activity in the right hemisphere should be interpreted with caution.

Nonetheless, our results clearly show a difference in TEP amplitudes as a function of visual feedback during movement control, which we interpret to reflect differences in effective connectivity. Furthermore, we have found a clear relationship between directed coherence, measured by MVAR models, and TEP-based measures of effective connectivity. Taken together, these results support the validity of using TEPs to measure changes in effective connectivity as a result of visual feedback of motor control. This could further establish TEPs as an accurate means of delineating region-region maps of effective connectivity differences in a variety of cogntivie tasks, which can in turn be used to identify network-based features relevant to cognition (Rogasch and Fitzgerald 2013, Ozdemir *et al* 2020) and neuropsychiatric disorders (Hampson and Hoffman 2010).

Data availability statement

The data cannot be made publicly available upon publication due to legal restrictions preventing unrestricted public distribution. The data that support the findings of this study are available upon reasonable request from the authors.

Conflict of interest

The authors declare no conflict of interest.

ORCID iDs

Ian Daly https://orcid.org/0000-0001-5489-0393
Nitin Williams https://orcid.org/0000-0002-0719-4616

References

Arai N, Lu M-K, Ugawa Y and Ziemann U 2012 Effective connectivity between human supplementary motor area and primary motor cortex: a paired-coil TMS study *Exp. Brain Res.* **220** 79–87

Astolfi L *et al* 2007 Comparison of different cortical connectivity estimators for high-resolution EEG recordings *Hum. Brain Mapp.* **28** 143–57

Awada K A, Jackson D R, Williams J T, Wilton D R, Baumann S B and Papanicolaou A C 1997 Computational aspects of finite element modeling in EEG source localization *IEEE Trans. Biomed. Eng.* **44** 736–52

Baccala L A and Sameshima K 2001 Partial directed coherence: a new concept in neural structure determination *Biol. Cybern.* **84** 463–74

Baccala L A, Sameshima K and Takahashi D Y 2007 Generalized partial directed coherence *2007 15th Int. Conf. on Digital Signal Processing, DSP 2007* pp 163–6

Baumann S B, Wozny D R, Kelly S K and Meno F M 1997 The electrical conductivity of human cerebrospinal fluid at body temperature *IEEE Trans. Biomed. Eng.* **44** 220–3

Belardinelli P *et al* 2019 Reproducibility in TMS–EEG studies: a call for data sharing, standard procedures and effective experimental control *Brain Stimul.* **12** 787–90

Belouchrani A, Belouchrani A, Abed-meraim K, Cardoso J F and Moulines E 1993 Second order blind separation of temporally correlated sources (available at: http://citeseerx.ist.psu.edu/viewdoc/summary?doi = 10.1.1.54.1662)

Benjamini Y and Hochberg Y 1995 Controlling the false discovery rate: a practical and powerful approach to multiple testing *J. R. Stat. Soc.* B **57** 289–300

Biabani M, Fornito A, Mutanen T P, Morrow J and Rogasch N C 2019 Characterizing and minimizing the contribution of sensory inputs to TMS-evoked potentials *Brain Stimul.* **12** 1537–52

Bonato C, Miniussi C and Rossini P 2006 Transcranial magnetic stimulation and cortical evoked potentials: a TMS/EEG co-registration study *Clin. Neurophysiol.* **117** 1699–707

Bortoletto M, Veniero D, Thut G and Miniussi C 2015 The contribution of TMS-EEG coregistration in the exploration of the human cortical connectome *Neurosci. Biobehav. Rev.* **49** 114–24

Braga R M, Fu R Z, Seemungal B M, Wise R J S and Leech R 2016 Eye movements during auditory attention predict individual differences in dorsal attention network activity *Front. Hum. Neurosci.* **10** 164

Breveglieri R, Borgomaneri S, Filippini M, Vitis M D, Tessari A and Fattori P 2021 Functional connectivity at rest between the human medial posterior parietal cortex and the primary motor cortex detected by paired-pulse transcranial magnetic stimulation *Brain Sci.* **11** 1357

Button K S, Ioannidis J P, Mokrysz C, Nosek B A, Flint J, Robinson E S and Munafò M R 2013 Power failure: why small sample size undermines the reliability of neuroscience *Nat. Rev. Neurosci.* **14** 365–76

Casarotto S, Lauro L J, Bellina V, Casali A G, Rosanova M, Pigorini A, Defendi S, Mariotti M and Massimini M 2010 EEG responses to TMS are sensitive to changes in the perturbation parameters and repeatable over time *PLoS One* **5** e10281

Casula E P, Tarantino V, Basso D, Arcara G, Marino G, Toffolo G M, Rothwell J C and Bisiacchi P S 2014 Low-frequency rTMS inhibitory effects in the primary

motor cortex: insights from TMS-evoked potentials *NeuroImage* **98** 225–32
Cheung B L P, Riedner B A, Tononi G and Veen B D V 2010 Estimation of cortical connectivity from EEG using state-space models *IEEE Trans. Biomed. Eng.* **57** 2122–34
Chung J W, Ofori E, Misra G, Hess C W and Vaillancourt D E 2017 Beta-band activity and connectivity in sensorimotor and parietal cortex are important for accurate motor performance *NeuroImage* **144** 164–73
Conde V, Tomasevic L, Akopian I, Stanek K, Saturnino G B, Thielscher A, Bergmann T O and Siebner H R 2019 The non-transcranial TMS-evoked potential is an inherent source of ambiguity in TMS-EEG studies *NeuroImage* **185** 300–12
Daly I, Blanchard C and Holmes N 2018 Cortical excitability correlates with the event-related desynchronization during brain-computer interface control *J. Neural Eng.* **15** 026022
Darmani G and Ziemann U 2019 Pharmacophysiology of TMS-evoked EEG potentials: a mini-review *Brain Stimul.* **12** 829–31
Desideri D, Zrenner C, Ziemann U and Belardinelli P 2019 Phase of sensorimotor μ-oscillation modulates cortical responses to transcranial magnetic stimulation of the human motor cortex *J. Physiol.* **597** 5671–86
Ding M, Bressler S L, Yang W and Liang H 2000 Short-window spectral analysis of cortical event-related potentials by adaptive multivariate autoregressive modeling: data preprocessing, model validation and variability assessment *Biol. Cybern.* **83** 35–45
Farzan F and Bortoletto M 2022 Identification and verification of a 'true' TMS evoked potential in TMS-EEG *J. Neurosci. Methods* **378** 109651
Ferreri F, Pasqualetti P, Määttä S, Ponzo D, Ferrarelli F, Tononi G, Mervaala E, Miniussi C and Rossini P M 2011 Human brain connectivity during single and paired pulse transcranial magnetic stimulation *NeuroImage* **54** 90–102
Freedberg M, Reeves J A, Hussain S J, Zaghloul K A and Wassermann E M 2020 Identifying site- and stimulation-specific TMS-evoked EEG potentials using a quantitative cosine similarity metric *PLoS One* **15** e0216185
Geddes L A and Baker L E 1967 The specific resistance of biological material-a compendium of data for the biomedical engineer and physiologist *Med. Biol. Eng.* **5** 271–93
Granö I, Mutanen T P, Tervo A, Nieminen J O, Souza V H, Fecchio M, Rosanova M, Lioumis P and Ilmoniemi R J 2022 Local brain-state dependency of effective connectivity: a pilot TMS-EEG study [version 2; peer review: 2 approved] *Open Res. Eur.* **2** 45
Grech R, Cassar T, Muscat J, Camilleri K P, Fabri S G, Zervakis M, Xanthopoulos P, Sakkalis V and Vanrumste B 2008 Review on solving the inverse problem in EEG source analysis *J. NeuroEng. Rehabil.* **5** 25
Hallett M 2000 Transcranial magnetic stimulation and the human brain *Nature* **406** 147–50
Hallett M 2007 Transcranial magnetic stimulation: a primer *Neuron* **55** 187–99
Hallett M, Iorio R D, Rossini P M, Park J E, Chen R, Celnik P, Strafella A P, Matsumoto H and Ugawa Y 2017 Contribution of transcranial magnetic stimulation to assessment of brain connectivity and networks *Clin. Neurophysiol.* **128** 2125–39
Hallez H *et al* 2007 Review on solving the forward problem in EEG source analysis *J. NeuroEng. Rehabil.* **4** 46
Hampson M and Hoffman R E 2010 Transcranial magnetic stimulation and connectivity mapping: tools for studying the neural bases of brain disorders *Front. Syst. Neurosci.* **4** 40
Haufe S, Tomioka R, Nolte G, Müller K R and Kawanabe M 2010 Modeling sparse connectivity between underlying brain sources for EEG/MEG *IEEE Trans. Biomed. Eng.* **57** 1954–63
Hernandez-Pavon J C, Kugiumtzis D, Zrenner C, Kimiskidis V K and Metsomaa J 2022 Removing artifacts from TMS-evoked EEG: a methods review and a unifying theoretical framework *J. Neurosci. Methods* **376** 109591
Hernandez-Pavon J C *et al* 2023 TMS combined with EEG: recommendations and open issues for data collection and analysis *Brain Stimul.* **16** 567–93
Ilmoniemi R J, Virtanen J, Ruohonen J, Karhu J, Aronen H J, Näätänen R and Katila T 1997 Neuronal responses to magnetic stimulation reveal cortical reactivity and connectivity *Neuroreport* **8** 3537–40
Janssens S E and Sack A T 2021 Spontaneous fluctuations in oscillatory brain state cause differences in transcranial magnetic stimulation effects within and between individuals *Front. Hum. Neurosci.* **15** 12
Kafashan M, Lepage K Q and Ching S 2014 Node selection for probing connections in evoked dynamic networks *Proc. IEEE Conf. on Decision and Control* pp 6080–5
Kaminski M and Blinowska K J 2014 Directed transfer function is not influenced by volume conduction-inexpedient pre-processing should be avoided *Front. Comput. Neurosci.* **8** 61
Keil J, Timm J, SanMiguel I, Schulz H, Obleser J and Schönwiesner M 2014 Cortical brain states and corticospinal synchronization influence TMS-evoked motor potentials *J. Neurophysiol.* **111** 513–9
Kerwin L J, Keller C J, Wu W, Narayan M and Etkin A 2018 Test-retest reliability of transcranial magnetic stimulation EEG evoked potentials *Brain Stimul.* **11** 536–44
Komssi S *et al* 2002 Ipsi- and contralateral EEG reactions to transcranial magnetic stimulation *Clin. Neurophysiol.* **113** 175–84
Kriegeskorte N, Simmons W K, Bellgowan P S and Baker C I 2009 Circular analysis in systems neuroscience: the dangers of double dipping *Nat. Neurosci.* **12** 535–40
Lepage K Q, Ching S and Kramer M A 2013 Inferring evoked brain connectivity through adaptive perturbation *J. Comput. Neurosci.* **34** 303–18
Mancuso M *et al* 2021 Transcranial evoked potentials can be reliably recorded with active electrodes *Brain Sci.* **11** 145
Murre J and Sturdy D 1995 The connectivity of the brain: multi-level quantitative analysis *Biol. Cybern.* **73** 529–45
Nicolaou N and Georgiou J 2013 Autoregressive model order estimation criteria for monitoring awareness during anaesthesia *IFIP Advances in Information and Communication Technology* vol 412 (Springer) pp 71–80
Nikulin V V, Kičić D, Kähkönen S and Ilmoniemi R J 2003 Modulation of electroencephalographic responses to transcranial magnetic stimulation: evidence for changes in cortical excitability related to movement *Eur. J. Neurosci.* **18** 1206–12
Noble J W, Eng J J and Boyd L A 2013 Effect of visual feedback on brain activation during motor tasks: an FMRI study *Motor Control* **17** 298–312
Noda Y 2020 Toward the establishment of neurophysiological indicators for neuropsychiatric disorders using transcranial magnetic stimulation-evoked potentials: a systematic review *Psychiatry Clin. Neurosci.* **74** 12–34
Oostenveld R, Fries P, Maris E and Schoffelen J-M 2011 FieldTrip: open source software for advanced analysis of MEG, EEG and invasive electrophysiological data *Comput. Intell. Neurosci.* **2011** 156869
Ozdemir R A, Tadayon E, Boucher P, Momi D, Karakhanyan K A, Fox M D, Halko M A, Pascual-Leone A, Shafi M M and Santarnecchi E 2020 Individualized perturbation of the human connectome reveals reproducible biomarkers of network dynamics relevant to cognition *Proc. Natl Acad. Sci. USA* **117** 8115–25
Raichle M E 2011 The restless brain *Brain Connect.* **1** 3–12
Rocchi L, Santo A D, Brown K, Ibáñez J, Casula E, Rawji V, Lazzaro V D, Koch G and Rothwell J 2021 Disentangling EEG responses to TMS due to cortical and peripheral activations *Brain Stimul.* **14** 4–18
Rogasch N C and Fitzgerald P B 2013 Assessing cortical network properties using TMS-EEG *Hum. Brain Mapp.* **34** 1652–69

Rogasch N C, Thomson R H, Farzan F, Fitzgibbon B M, Bailey N W, Hernandez-Pavon J C, Daskalakis Z J and Fitzgerald P B 2014 Removing artefacts from TMS-EEG recordings using independent component analysis: importance for assessing prefrontal and motor cortex network properties *NeuroImage* **101** 425–39

Rogasch N C, Biabani M and Mutanen T P 2022 Designing and comparing cleaning pipelines for TMS-EEG data: a theoretical overview and practical example *J. Neurosci. Methods* **371** 109494

Rosanova M, Casali A, Bellina V, Resta F, Mariotti M and Massimini M 2009 Natural frequencies of human corticothalamic circuits *J. Neurosci.* **29** 7679–85

Rossi S, Hallett M, Rossini P M and Pascual-Leone A 2009 Safety, ethical considerations and application guidelines for the use of transcranial magnetic stimulation in clinical practice and research *Clin. Neurophysiol.* **120** 2008–39

Rossini P *et al* 2015 Non-invasive electrical and magnetic stimulation of the brain, spinal cord, roots and peripheral nerves: basic principles and procedures for routine clinical and research application. an updated report from an i.f.c.n. committee *Clin. Neurophysiol.* **126** 1071–107

Rothwell J C 2011 Using transcranial magnetic stimulation methods to probe connectivity between motor areas of the brain *Hum. Mov. Sci.* **30** 906–15

Rubinov M and Sporns O 2009 Complex network measures of brain connectivity: uses and interpretations *NeuroImage* **52** 1059–69

Sasaki K, Fujishige Y, Kikuchi Y and Odagaki M 2021 A transcranial magnetic stimulation trigger system for suppressing motor-evoked potential fluctuation using electroencephalogram coherence analysis: algorithm development and validation study *JMIR Biomed. Eng.* **6** e28902

Schaworonkow N, Triesch J, Ziemann U and Zrenner C 2019 EEG-triggered TMS reveals stronger brain state-dependent modulation of motor evoked potentials at weaker stimulation intensities *Brain Stimul.* **12** 110–8

Siebner H R, Conde V, Tomasevic L, Thielscher A and Bergmann T O 2019 Distilling the essence of TMS-evoked EEG potentials (TEPs): a call for securing mechanistic specificity and experimental rigor *Brain Stimul.* **12** 1051–4

Sporns O 2007 Brain connectivity *Scholarpedia* **2** 4695

Stancak A and Pfurtscheller G 1996 Event-related desynchronisation of central beta-rhythms during brisk and slow self-paced finger movements of dominant and nondominant hand *Cogn. Brain Res.* **4** 171–83

ter Braack E M, de Vos C C and van Putten M J 2015 Masking the auditory evoked potential in TMS–EEG: a comparison of various methods *Brain Topogr.* **28** 520–8

Theodoridis S and Koutroumbas K 2006 *Pattern Recognition* (Elsevier/Academic) p 837

Thut G, Ives J R, Kampmann F, Pastor M A and Pascual-Leone A 2005 A new device and protocol for combining TMS and online recordings of EEG and evoked potentials *J. Neurosci. Methods* **141** 207–17

Varone G, Hussain Z, Sheikh Z, Howard A, Boulila W, Mahmud M, Howard N, Morabito F C and Hussain A 2021 Real-time artifacts reduction during TMS-EEG co-registration: a comprehensive review on technologies and procedures *Sensors* **21** 637

Veniero D, Bortoletto M and Miniussi C 2009 TMS-EEG co-registration: on TMS-induced artifact *Clin. Neurophysiol.* **120** 1392–9

Vink J, Westover M, Pascual-Leone A and Shafi M 2017 EEG functional connectivity predicts propagation of TMS-evoked potentials *Brain Stimul.* **10** 516

Vink J, Westover M, Pascual-Leone A and Shafi M 2019 EEG functional connectivity predicts causal brain interactions *Brain Stimul.* **12** 449

Wang Z, Bovik A C, Sheikh H R and Simoncelli E P 2004 Image quality assessment: from error visibility to structural similarity *IEEE Trans. Image Process.* **13** 600–12

Williams N, Daly I and Nasuto S 2018 Markov model-based method to analyse time-varying networks in EEG task-related data *Front. Comput. Neurosci.* **12** 76

Wolters C H, Köstler H, Möller C, Härdtlein J, Grasedyck L and Hackbusch W 2007 Numerical mathematics of the subtraction method for the modeling of a current dipole in EEG source reconstruction using finite element head models *SIAM J. Sci. Comput.* **30** 24–45

Yamanaka K, Kadota H and Nozaki D 2013 Long-latency TMS-evoked potentials during motor execution and inhibition *Front. Hum. Neurosci.* **7** 11

Yeom H G, Kim J S and Chung C K 2020 Brain mechanisms in motor control during reaching movements: transition of functional connectivity according to movement states *Sci. Rep.* **10** 1–11

Ziluk A, Premji A and Nelson A J 2010 Functional connectivity from area 5 to primary motor cortex via paired-pulse transcranial magnetic stimulation *Neurosci. Lett.* **484** 81–85